Available online at www.sciencedirect.com
SCIENCE DIRECT®
Journal of Nuclear Materials 350 (2006) 147–152
journal of nuclear materials
www.elsevier.com/locate/jnucmat

Nanoindentation characterization of ErT_2 thin films

J.A. Knapp *, J.F. Browning

Sandia National Laboratories, P.O. Box 5800, Albuquerque, NM 87185-1056, United States

Received 26 July 2005; accepted 23 November 2005

Abstract

The properties of ErT_2 films change as the tritium decays into ^3He, which has important implications for long-term film stability in applications such as neutron generators. Ultra-low load nanoindentation, analyzed using finite-element modeling to separate the nanomechanical properties of 500 nm ErT_2 layers from those of the underlying substrates, has been used to examine the films as they age. The ^3He bubbles which form as the film ages act as barriers to dislocation movement, hardening the material, but not dramatically affecting the elastic properties. By modeling the layer as an isotropic, elastic–plastic solid with the Mises yield criterion, the nanoindentation data is shown to correspond to an increase of nearly 2× in strength after aging for over a year.

PACS: 62.20.−x; 61.80.−x; 81.40.Cd; 28.52.Fa

1. Introduction

The mechanical properties of metals containing dispersions of small gas bubbles are of fundamental interest for understanding the effects of nanometer-sized inclusions on strength. They are also very important in applying materials to applications involving tritium, such as neutron tubes, which are neutron-generating devices that use metal tritide films. The tritium slowly decays into ^3He, which is either released from the film, leading to vacuum problems in a sealed tube, or, if retained, forms high pressure bubbles that may eventually fracture the film. Not only are the conditions leading to fracture of interest, but the mechanical properties of the layer before fracture are of fundamental importance for understanding how to control early ^3He release. In the study presented here, we are using fully tritiated ErT_2 model films to study the property changes to be expected for an aging neutron tube target film. We present nanomechanical measurements only; details of microstructural characterization will be given elsewhere.

Quantifying the mechanical properties of thin films is a difficult, but increasingly important task as thin films are used in a wide variety of applications. Instrumented indentation, commonly termed

* Corresponding author. Tel.: +1 505 844 2305; fax: +1 505 844 7775.
E-mail address: jaknapp@sandia.gov (J.A. Knapp).

0022-3115/$ - see front matter © 2006 Elsevier B.V. All rights reserved.
doi:10.1016/j.jnucmat.2005.11.018

nanoindentation, can be used for such measurements, but interpreting the data to extract mechanical properties becomes difficult for deposited layers on the order of a micron or less in thickness, where the properties of the underlying substrate bias the results in a way that cannot be easily accounted for using analytical methods [1–4]. We have approached the problem of evaluating thin layer mechanical properties by using finite-element computer simulations to model the nanoindentation experiment in as much detail as possible, varying the unknown properties of just the layer until a match to experiment is obtained [5–10]. For these studies, we repeat the measurements at approximately 30 day intervals.

2. Sample preparation

The specimens were prepared as part of a large, parallel set of samples, with others of the set being examined with electron microscopy, X-ray diffraction, and neutron scattering as the samples age [11]. In order to provide specimens as flat as possible, Si(1 0 0) wafers were used as the substrate, with a nominal 100 nm layer of Mo deposited on top to prevent the formation of Er–Si compounds during the hydriding process. Er was deposited by electron beam physical vapor deposition to a thickness of 500 nm at Sandia National Laboratories, and subsequently loaded to the dihydride phase with 100% T at the Los Alamos National Laboratory Tritium Science and Engineering Facility. After loading, the ErT_2 films were somewhat rougher because of the phase change, and 10% thicker. Ion beam analysis was used to determine tritium and erbium areal densities while X-ray diffraction was performed to verify the films had been loaded to the dihydride phase. For the nanomechanical measurements, three of the samples were permanently glued onto a sample puck for mounting in the indenter. The samples, with puck, are kept under vacuum between measurements; each set of indentations exposes the samples to air for 7–8 h.

3. Nanoindentation and finite-element modeling

An important consideration for measuring the properties of tritiated samples is the necessity for safety controls to prevent the possible spread of tritium contamination or exposure to personnel. Although our laboratory has a tritium facility with several rooms dedicated to tritium handling with engineering controls to contain accidental releases, the instrument we use for nanoindentation is in a separate building. We devised a procedure using a removable, dedicated sample stage with a replaceable bag which surrounds and seals off the indenter tip fixture and the sample during indents, such that any release of particles from the sample during an indent would be contained. The samples are mounted and dismounted from the stage using a hood in the tritium handling facility, and remain within the bag during transport between buildings and measurement. Areas around the indenter are surveyed for contamination after each set of measurements. The instrument we use is an MTS Nano Indenter XP, fitted with the continuous stiffness measurement option and a nanopositioning stage [12].

Each set of measurements consists of 8–10 indents to a depth of 200 nm on each of the three samples, along with calibration indents in fused silica mounted alongside. Additional sets of indents are sometimes obtained if the data show exceptional scatter due to local roughness. The indent data is obtained using the continuous stiffness measurement technique (CSM) [2], which imposes a small oscillation ($\pm$1 nm) on the indent depth control to obtain both loading force and sample stiffness as a continuous function of depth into the sample. The shape of the dedicated tip is re-calibrated for each run, using the indent data from silica and images of a residual indent to determine the mounting angle of the tip (which can vary somewhat each time the tip is re-mounted) [4].

Interpreting the data obtained directly from nanoindentation is difficult for thin films because the properties of the underlying substrate can strongly influence the results in a way that cannot be accounted for using analytical methods [1–4]. In this case the problem is compounded, since the substrate consists of both Si(1 0 0) and a thin layer of Mo. For the analysis, we use an approach that we have used in a wide variety of thin film studies [5–10]. The experiment is simulated as closely as possible using finite-element modeling (FEM), matching the mesh to the measured layer thicknesses and tip shape, and fixing the material properties of substrate and tip to previously measured values while varying only the properties of the unknown layer. The results of the simulations are compared to the data over the range of 40–50 nm through the end of the indent; this range avoids the shallow portion of the indent where the transition to plasticity takes place and

where thin oxides might skew the results. A series of simulations is performed until an acceptably close match to the experimental data over this range is obtained, and the properties of the layer material are taken to be those that give the best fit. Although a modeling approach requires some approximations and cannot determine some properties such as the coefficient of work hardening, the technique gives reasonably quantitative results and is especially useful for comparative studies on similar material, as here.

The modeling proceeds by first defining a two-dimensional axisymmetric mesh using the measured layer thicknesses and the separately determined area function of the indenter. A time-independent, isotropic, elastic–plastic constitutive model with the Mises yield criterion is used for all materials. The isotropic model allows us to specify the mechanical response of each material with Poisson's ratio and a simple stress–strain curve, parameterized by Young's modulus E, yield stress Y, and a work hardening exponent. Each work hardening exponent must be estimated in the absence of additional information such as a measurement of the pileup around the indents, and here the work hardening exponent for ErT_2 is taken to be 0.25, a value typical of many non-brittle materials. The choice of work hardening exponent influences the deduced value of Y but has little effect on the inferred hardness or Young's modulus. An average value of 0.25 is assumed for the Poisson's ratio for ErT_2 (which also has little influence on the results). To properly account for the substrate, we first separately indented the Si(1 0 0) substrate and then the Si with the Mo layer, using the modeling to determine the mechanical response of both the Si and the Mo. These are then fixed in all following simulations for the combined structure with ErT_2. Finally, Y and E for just the ErT_2 layer in each sample is varied in a series of FEM simulations using ABAQUS/Standard [13] until a close fit to the experimental data is obtained.

The procedure above gives a yield strength and Young's modulus for the material, using the assumed work hardening. The simulations do not directly give a hardness of the layer material, since they still include the substrate, so in order to obtain a value for hardness for the layer material alone, an additional calculation is required, where the stress–strain curve for the material is used in a simulation of an indent into a bulk sample. The hardness for the material, defined as the loading force divided by projected contact area, is then obtained directly from this final simulation.

4. Results

Fig. 1 shows both experimental data and best-fit simulations for three samples, with load versus depth in panel (a) and stiffness versus depth in panel (b). In each case the solid line is the simulation and the symbols are averages of 8–10 indents, with error bars indicating the standard deviation of the average values. The Er metal was indented to 160 nm, while ErT_2 and ErD_2 layers were indented to 200 nm. The curves with open squares are the data obtained from Er metal before loading, and the fit gives a yield strength of $Y = 0.15 \pm 0.04$ GPa, Young's modulus $E = 77 \pm 12$ GPa, and hardness $H = 1.9 \pm 0.4$ GPa. The errors are estimated in each

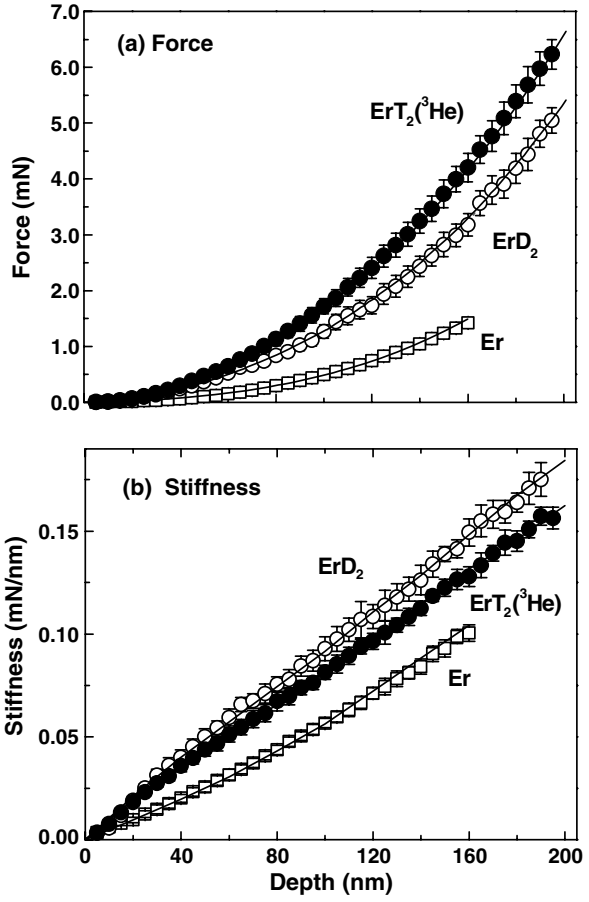

Fig. 1. (a) Indentation force versus depth for Er metal, ErD_2, and ErT_2 aged for 408 days. Symbols are experimental data, while the solid lines are from the best-fit FEM simulations for each set of data. (b) Indentation stiffness versus depth for the same samples.

case based on both the spread in the experimental results and the quality of the numerical fit to the data. The hardness we obtain here is higher than reported in the literature for bulk Er metal, but the modulus is close to the literature value of 69.9 GPa [14,15]. This deposited Er layer is probably somewhat finer grained and hence harder than typical bulk samples.

For determining the properties of the hydride phase without the complication of tritium decay, a sample was loaded with 100% deuterium to the ErD_2 phase. The indentation results for this sample are shown by the open circle symbols in Fig. 1. Both load and stiffness are substantially higher than for Er at all depths and the fitting gives $Y = 1.12 \pm 0.19$ GPa, $E = 175 \pm 15$ GPa, and hardness $H = 5.5 \pm 0.7$ GPa. The modulus is much higher and the layer is over twice as hard as the Er metal.

The final example in Fig. 1 is a set of data and the fit for an ErT_2 sample measured at 408 days after loading with 100% tritium. If all of the ^{3}He were retained in the sample, the composition would be approximately 4.1% ^{3}He, with more than 6% of the ErT_2 converted to Er. The raw experimental data, indicated by the filled circles, shows a higher loading force but somewhat reduced stiffness compared to the ErD_2 layer. Intuitively, this would seem to indicate a lowered modulus and somewhat higher strength. The modeling, however, shows that although the sample is substantially harder, the modulus is essentially unchanged. The numbers are $Y = 2.35 \pm 0.33$ GPa, $E = 170 \pm 12$ GPa, and hardness $H = 9.0 \pm 0.9$ GPa. This is a case that illustrates the value of the modeling approach, since details like the area in contact at a given depth are accounted for. Here, the harder sample has less area in contact with the indenter at a given depth, which in turn reduces the measured stiffness slightly, even though the elastic properties are essentially unchanged.

A summary of measured hardness for these samples as a function of approximate ^{3}He content is shown in Fig. 2, with the time after loading shown at the top for the ErT_2 samples. The ^{3}He content scale is calculated assuming that all ^{3}He produced by tritium decay is retained in the layer. Results for the ErD_2 layer are shown at the left, at 0% ^{3}He. There are no measurements for ErT_2 near zero age for practical reasons of sample transfer, so the measurements of ErD_2 are taken to be representative of ErT_2 immediately upon loading. This should be a reasonable approximation, although there may

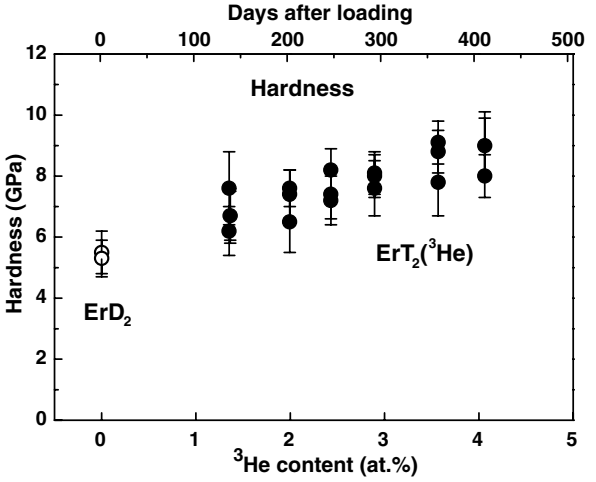

Fig. 2. Material hardness determined by FEM modeling of indentation data for ErD_2 and aged ErT_2.

be some differences due to different loading systems used for the two gases. As shown in Fig. 1, the hardness increases monotonically as the samples age. The filled circles are the data from the aging ErT_2 samples, obtained from 133 days after loading through 408 days. At each age, three points are shown, one from each sample. The variation between samples are attributed to surface roughness and to local differences in grain orientation. Even with the variation, it is clear that the hardness is trending up with age, with no clear indication of a plateau after a year.

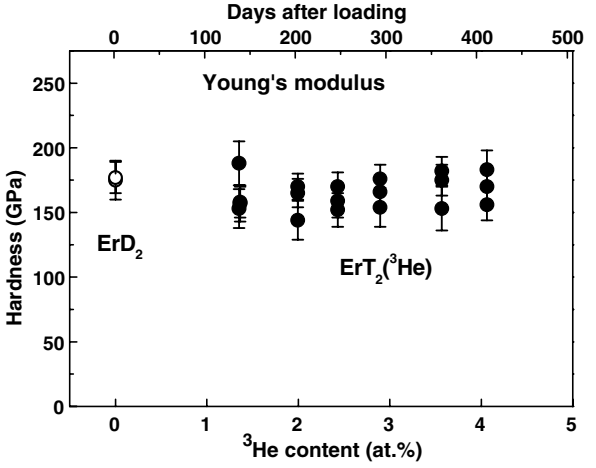

Fig. 3. Young's modulus determined by FEM modeling of indentation data for ErD_2 and aged ErT_2.

Table 1
Mechanical properties of ErD_2 and ErT_2 layers

Sample	Days after load	^{3}He (at.%)	Yield (GPa)	Young's modulus (GPa)	Hardness (GPa)
ErD_2	0	0	1.12 ± 0.19	175 ± 15	5.5 ± 0.7
ErD_2	0	0	1.08 ± 0.17	177 ± 12	5.3 ± 0.6
ErT_2A	133	1.35	1.74 ± 0.38	188 ± 17	7.6 ± 1.2
ErT_2B	133	1.35	1.40 ± 0.25	153 ± 15	6.2 ± 0.8
ErT_2B	134	1.36	1.58 ± 0.26	157 ± 14	6.7 ± 0.9
ErT_2C	134	1.36	1.57 ± 0.27	158 ± 12	6.7 ± 0.8
ErT_2A	197	1.99	1.81 ± 0.16	170 ± 10	7.6 ± 0.6
ErT_2B	197	1.99	1.78 ± 0.28	165 ± 11	7.4 ± 0.8
ErT_2C	197	1.99	1.57 ± 0.30	144 ± 15	6.5 ± 1.0
ErT_2A	241	2.43	1.79 ± 0.22	159 ± 13	7.4 ± 0.8
ErT_2B	241	2.43	1.79 ± 0.23	152 ± 13	7.2 ± 0.8
ErT_2C	241	2.43	2.05 ± 0.22	170 ± 11	8.2 ± 0.7
ErT_2A	288	2.89	1.97 ± 0.20	176 ± 11	8.1 ± 0.7
ErT_2B	288	2.89	1.89 ± 0.26	154 ± 15	7.6 ± 0.9
ErT_2C	288	2.89	1.99 ± 0.21	166 ± 11	8.0 ± 0.7
ErT_2A	357	3.57	1.99 ± 0.32	153 ± 17	7.8 ± 1.1
ErT_2B	357	3.57	2.21 ± 0.18	175 ± 12	8.8 ± 0.7
ErT_2C	357	3.57	2.31 ± 0.21	182 ± 11	9.1 ± 0.7
ErT_2A	408	4.06	2.02 ± 0.21	156 ± 12	8.0 ± 0.7
ErT_2B	408	4.06	2.26 ± 0.36	183 ± 15	9.0 ± 1.1
ErT_2C	408	4.06	2.35 ± 0.33	170 ± 12	9.0 ± 0.9

The increase in hardness with age is expected, as the increasing ^{3}He content forms platelet-like bubbles within the matrix [11] and these in turn harden the material, much like Orowan hardening by precipitates [10]. Unlike precipitates, at sufficiently high ^{3}He pressure the bubbles may cause fracture, leading to layer failure and delamination.

Fig. 3 shows the corresponding values of Young's modulus for the same samples as a function of age and approximate ^{3}He content. Unlike the hardness, the modulus is essentially unchanged after a year of T decay. This is perhaps surprising, as the He bubbles must change the elastic properties of the layer, but apparently the high-pressure bubbles are sufficiently stiff that the average elasticity is little changed, if at all. Table 1 summarizes the results for all these samples. The average modulus for all the measurements of ErT_2 is 165 GPa, which gives a shear modulus of 66 GPa, assuming an isotropic material and Poisson's ratio of 0.25.

These measurements are being continued and will soon be combined with direct ion beam analysis to determine the actual ^{3}He and T content of the films [16]. We expect to determine the maximum hardness that the material achieves before shear failure between bubbles leads to layer failure. Examining similar layers with alloying or precipitate strengthening may lead to engineering solutions for controlling He release, both early release and ultimate layer failure.

Acknowledgements

Ion beam analysis by James Banks, X-ray diffraction by Mark Rodriguez, and technical assistance with radiation safety issues by Eric Staab are all gratefully acknowledged. Sandia National Laboratories is a multi-program laboratory operated by Sandia Corporation, a Lockheed Martin Company, for the United States Department of Energy's National Nuclear Security Administration under contract DE-AC04-94AL85000.

References

[1] G.M. Pharr, W.C. Oliver, MRS Bull. 17 (1992) 28.
[2] W.C. Oliver, G.M. Pharr, J. Mater. Res. 7 (1992) 1564.
[3] M.F. Doerner, W.D. Nix, J. Mater. Res. 1 (1986) 601.
[4] W.C. Oliver, G.M. Pharr, J. Mater. Res. 19 (2004) 3.
[5] J.A. Knapp, S.M. Myers, D.M. Follstaedt, G.A. Petersen, J. Appl. Phys. 86 (1999) 6547.
[6] J.A. Knapp, D.M. Follstaedt, S.M. Myers, J.C. Barbour, T.A. Friedmann, J. Appl. Phys. 85 (1999) 1460.
[7] J.A. Knapp, D.M. Follstaedt, S.M. Myers, J.C. Barbour, T.A. Friedmann, J.W. Ager, O.R. Monteiro, I.G. Brown, Surf. Coat. Technol. 104 (1998) 268.
[8] S.M. Myers, J.A. Knapp, D.M. Follstaedt, M.T. Dugger, J. Appl. Phys. 83 (1998) 1256.

[9] J.A. Knapp, D.M. Follstaedt, J.C. Barbour, S.M. Myers, Nucl. Instrum. and Meth. B 127 (1997) 935.
[10] J.A. Knapp, D.M. Follstaedt, S.M. Myers, Int. J. Damage Mech. 12 (2003) 377.
[11] J.F. Browning, et al., in preparation.
[12] Nano Instruments Innovation Center, MTS Systems Corp., Knoxville, TN, United States.
[13] ABAQUS version 6.3, Hibbitt, Karlsson and Sorensen, Inc., Pawtucket, RI.
[14] C.V. Owen, T.E. Scott, J. Less-Common Met. 16 (1968) 447.
[15] Metals Handbook, ASM, Metals Park, Ohio, 1990 (2), p. 1180.
[16] J.A. Knapp, K. Arstila, W.R. Wampler, J.C. Banks, B.L. Doyle, Nucl. Instrum. and Meth. B 219–220 (2004) 440.